

## Computational Discovery of an AI-Driven Dexamethasone Derivative for Parkinson's disease: Network Pharmacology, Docking, and MD Simulations

Mohammed M. Alshehri<sup>1,2</sup>, Nemat Ali<sup>4\*</sup>, Ahmed F. Alanazi<sup>1,2</sup>, Abdullah M. Albogami<sup>1,2</sup>, Nasser Gazy Almanea<sup>1,2</sup>, Falah Muslat Alsubaie<sup>1,2</sup>, Farhan Ali Alanazi<sup>3</sup>, Ahmed Salem Alharbi<sup>5</sup>, Abdulaziz Adel Alshamsi<sup>5</sup>, Musab Saeed Khamisah<sup>5</sup> & Faisal Abdulaziz Alwashmi<sup>5</sup>

<sup>1</sup>Pharmaceutical Care Department, Ministry of National Guard-Health Affairs, Riyadh, Saudi Arabia

<sup>2</sup>King Abdullah International Medical Research Center, Ministry of National Guard-Health Affairs, Riyadh 14611, Saudi Arabia

<sup>3</sup>Department of Medical Supply, Rafha Maternity and Children Hospital, Northern Borders Health Cluster, Ministry of Health, Rafha, Saudi Arabia

<sup>4</sup>Department of Pharmacology and Toxicology, College of Pharmacy, King Saud University, Riyadh, Saudi Arabia

<sup>5</sup>Department of Emergency Medicine, Ministry of National Guard-Health Affairs, Saudi Arabia

*Received 17 September 2025; revised 6 December 2025*

Parkinson's disease (PD) is a complex neurodegenerative disorder with few treatment options that are responsible for only slowing the disease progression. Several studies observed that dexamethasone exhibits neuroprotective effects; however, its systemic side effects restrict its use for prolonged periods. Our study employed Webserver-Aided Drug Design by Artificial Intelligence and Classical Algorithm (WDDAICA) to generate novel dexamethasone analogues with improved pharmacological properties suitable for PD therapy. Differentially expressed genes (DEGs) from the transcriptome data of PD patients (GSE160299) have been compared with dexamethasone-responsive genes, resulting in the identification of 92 shared targets. Enrichment analysis identified essential molecular functions, including metal ion binding and enzyme regulation, highlighting APOE, ICAM1, GAPDH, and EGF as critical targets. The AI-generated derivatives were evaluated using molecular docking against these targets, with molecule C displaying the best binding affinity to APOE (−7.6 kcal/mol), passing dexamethasone (−7.2 kcal/mol). ADMET profiling shows improved oral bioavailability and blood-brain barrier (BBB) permeability for molecule C; however, it also indicates elevated risk for hepatic damage. Molecular dynamics (MD) simulations validated enhanced structural stability and compactness of the molecule C–APOE complex. Additionally, MM-PBSA free energy assessments indicated a superior binding energy for molecule C (−13.8 kcal/mol) in contrast to dexamethasone (−1.8 kcal/mol), accompanied by more comprehensive per-residue interactions. The data indicates that molecule C may be an acceptable candidate for subsequent in vivo study as a neuroprotective drug in PD.

**Keywords:** Parkinson's disease; APOE; Dexamethasone; AI Drug Design; Molecular Dynamics Simulations

### Introduction

Parkinson's disease (PD) is a chronic neurological disease that defined by a fundamental spectrum of motor disorders, including bradykinesia, muscle rigidity, and tremor, with several non-motor manifestations such as anxiety, and dementia. From a global perspective, the burden of PD has been increasing significantly and according to the world health organization in 2023 the disability-adjusted life years due to PD have increased by 81% since 2000, and deaths have increased by > 100%. Decreased neurotransmitter levels, oxidative stress, dysfunction of mitochondria, and disrupted protein homeostasis exacerbate symptoms of PD over time<sup>1,2</sup>. The clinical characteristic of PD is Lewy bodies, which are

aggregates of misfolded  $\alpha$ -synuclein protein that result in the degeneration of the middle brain neurons that generate dopamine. In PD, APOE plays a regulatory role in neuroinflammation and dopaminergic neuronal death by creating a chronic immune activation. Activated microglia, the resident immune cells of the brain, respond by releasing large amounts of pro-inflammatory cytokines including tumor necrosis factor- $\alpha$  (TNF- $\alpha$ ), interleukin-1 $\beta$  (IL-1 $\beta$ ), and interleukin-6 (IL-6)<sup>3</sup>. Furthermore, inflammatory cytokines can activate NF- $\kappa$ B and MAPK pathways, upregulating apoptotic genes and amplifying local inflammation<sup>4</sup>. The exact cause of PD is unknown, however, targeting PD genes is emerging as a novel approach in disease progression and diagnosis. Plenty of research aimed in identifying causal factors and molecular markers of PD and distinguishing their gene functions between healthy and pathological states.

\*Correspondence:  
E-mail: nali1@ksu.edu.sa

Additionally, Gene mutations are especially crucial for familial and early-onset forms of PD, as they can disrupt essential cellular function leading to the gradual degeneration of dopaminergic neurons<sup>5</sup>. Management PD presents many difficulties due to its intricate and progressive nature, while current treatment options aim to mitigate symptoms and delay disease advancement. Artificial intelligence (AI) is transforming drug design and discovery, especially for complex neurodegenerative diseases such as PD. AI accelerates the identification of novel drug candidates by analyzing huge biological datasets to recognize patterns and predict drug-target interactions with specificity<sup>6</sup>. Dexamethasone, a potent synthetic glucocorticoid, has been studied regarding PD primarily for its anti-inflammatory properties. Preclinical studies suggest that dexamethasone may reduce dopaminergic neuronal degeneration in toxin-induced PD mice<sup>7</sup>. By activating the glucocorticoid receptor, dexamethasone suppresses the NF- $\kappa$ B and MAPK signaling pathways, thereby reducing the production of these cytokines and attenuating oxidative and excitotoxic damage. This anti-inflammatory modulation helps preserve dopaminergic neuron integrity and mitochondrial function, linking its immunosuppressive activity to neuroprotection in PD. Despite the promising nature of these findings, the extended use of dexamethasone is limited by its systemic side effects, including immunosuppression and metabolic disturbances<sup>8</sup>. The current study utilized AI-based molecular design to develop new dexamethasone derivatives, attempting to maintain neuroprotective characteristics while minimizing systemic side effects. To assess the therapeutic potential of these derivatives in relation to Parkinson's disease (PD), *in silico* experiments were performed targeting proteins encoded by genes identified as differentially expressed in PD patients, employing transcriptome data from the GEO dataset GSE160299. This dataset provides extensive gene expression profiles which are useful in identifying molecular targets involved in the origin of PD. The approach described here proposes to identify dexamethasone analogs with enhanced binding affinity and safety profiles for possible therapeutic applications in PD by integrating AI-assisted molecular synthesis. To achieve this, we docked dexamethasone and AI generated analogs against the hub genes on specific residues that could be responsible for the modulation by utilizing Protein Allosteric Sites Server (PASSer). Afterwards, molecules having best binding affinity were subjected for *in silico* ADME and toxicological properties. Finally, the protein-ligand complex stability

was studied through molecular dynamics simulation and free energy estimation using MM-PBSA.

## Materials and Methods

### Gene Data Sources

For identifying therapeutic targets associated with PD, genes with differential expression were identified from the GEO dataset GSE160299, which assesses plasma transcriptomes of PD patients and healthy controls. Plasma transcriptome data for PD target identification enables minimally invasive, scalable sampling while capturing circulating gene-expression signals linked to PD pathology. Recent study shows that plasma profiles can reflect PD-related transcriptional changes, and support biologically meaningful overlap between peripheral blood and brain pathways in PD<sup>9</sup>. A fold change threshold of  $\geq 3$  was employed to ensure high specificity and avoid inclusion of marginally altered transcripts. Although less stringent thresholds could identify additional DEGs, our focus was on capturing the genes with strong and biologically meaningful expression changes. A database of dexamethasone-responsive genes was acquired from the Comparative Toxicogenomics Database (CTD) (<https://ctdbase.org/>)<sup>10</sup> by entering "dexamethasone" inside of the "Chemicals" category to examine the association of these PD-associated genes with dexamethasone. The overlap of dexamethasone-associated and PD-related gene sets was depicted using the Draw Venn Diagram tool (<https://bioinfogp.cnb.csic.es/tools/venny/>)<sup>11</sup>. Genes identified in both datasets were regarded as potential targets of dexamethasone within the framework of PD. The overlapped genes were further functionally categorized utilizing the Enricher approach (accessed in May 2025) to ascertain their molecular activities, biological processes, and possible roles in PD-related signaling pathway<sup>12</sup>.

### Protein-Protein Interaction (PPI) Network Construction and Hub Gene Identification

To investigate the molecular pathways that could possibly underlying the advantageous effects of dexamethasone on PD, the overlap between PD-associated genes and dexamethasone target genes has been observed and classified as probable gene candidates. The officially recognized gene symbols of the intersecting genes have been posted to the STRING database (<https://string-db.org/>)<sup>13</sup> using the "Multiple Proteins" option, with the organism specification set to Homo sapiens. A protein-protein

interaction (PPI) network has been created utilizing established and predicted interactions. The resulting network was exported and visualized using Cytoscape software (version 3.10.1, Boston, MA, USA)<sup>14</sup>. Following that, network topological results were generated using the "Analyze Network" function in Cytoscape. The CytoHubba plugin was employed to identify critical genes for regulation within the network, selecting the top 20 genes based on their topological significance. These genes were recognized as hub genes that may enhance the interaction between dexamethasone and PD.

#### Gene ontology (GO) and functional enrichment analysis of hub genes

The identified symbols of the evaluated hub genes were submitted to the Database for Annotation, Visualization, and Integrated Discovery (DAVID) (<https://david.ncifcrf.gov/>)<sup>15,16</sup>, distinguishing the species as *Homo sapiens*. The "Functional Annotation Tool" was selected, with the "Gene Ontology" and "Reactome Pathway" option selected. GO enrichment analysis was performed over three distinct groups: Biological Processes (BP), Cellular Components (CC), and Molecular Functions (MF). The nine most significantly enriched terms ( $P < 0.05$ ) from each Gene Ontology category were chosen for display. Furthermore, Reactome pathway enrichment analysis was conducted, identifying the top 9 significantly enriched pathways ( $P < 0.05$ ). All enrichment outcomes were illustrated using bubble plots, created with the SRplot web program (<https://www.bioinformatics.com.cn/srplot/>)<sup>17</sup>.

#### AI dexamethasone modeling

WADDAICA (Webserver-Aided Drug Design by Artificial Intelligence and Classical Algorithm) is an AI-driven platform developed for the intelligent transformation of drugs in order to create structurally optimal variation. WADDAICA employs a hybrid methodology that combines deep learning models with conventional cheminformatics approaches for changing the pharmacophore of identified drugs. WADDAICA models trained on large chemical and protein–ligand datasets to generate novel molecular scaffolds. The program demanded input in the form of SMILES strings, which provide a concise and machine-readable representation of molecular structures. The canonical SMILES of dexamethasone have been obtained from the PubChem database (<https://pubchem.ncbi.nlm.nih.gov/>) and uploaded to WADDAICA. The program generated 10 candidate

molecules derived from the structural attributes and functional groups of dexamethasone<sup>18,19</sup>.

#### Ligand preparation

After AI modeling of dexamethasone, the structures of dexamethasone and AI derived molecules had been imported into PyRx 0.8 using the open Babel tool (version 3.1.1.). Then, crucial characteristics including element, hybridization, and connectivity were taken into consideration throughout the energy minimization process. As part of this procedure, the universal force field was employed<sup>20</sup>. This was followed by converting the ligands to PDBQT format, which is the typical format for AutoDock Ligands.

#### Protein target identification and preparation

Based on the results of the network pharmacology and protein-protein interaction analyses, four notable target proteins: ICAM1, GAPDH, EGF, and APOE, were chosen for further evaluation including molecular docking and dynamic simulation analyses. These proteins were chosen for their crucial roles in the interaction network between dexamethasone and PD. The three-dimensional structures of the selected proteins have been collected from the Protein Data Bank (PDB) (<https://www.rcsb.org/>): ICAM1 (PDB ID: 1MQ8), GAPDH (PDB ID: 1U8F), EGF (PDB ID: 1NQL), and APOE (PDB ID: 1B68). All heteroatoms, including water molecules, ions, and associated ligands, were removed from the protein structure to prepare it for molecular docking. Following that, the resulting structure was optimized for conservation of energy and any missing residues modeled using the Dunbrack rotamer library using molecular visualization using UCSF Chimera (version 1.13.1; <https://www.cgl.ucsf.edu/chimera/>). The level of accuracy of molecular docking and dynamic simulations may be compromised by steric disputes or unfavorable configurations; thus, this minimization phase proved crucial<sup>21</sup>.

#### Docking procedure and identification of protein allosteric site

The docking software PyRx 0.8<sup>22,23</sup>, was used to import the purified target structures. The "load molecule" option in the File toolbar was selected for this purpose. The receptor structure was then converted to an AutoDock macromolecule (PDBQT format) using the right-click option. PyRx 0.8's Vina Wizard Tool was additionally utilized to do binding affinity analyses. For docking, we used PDBQT files for both the ligands and the targets. For the molecular

docking, specific 3D grid boxes were established (size\_x = 21.211 Å, size\_y = 20.755 Å, and size\_z = 13.287 Å) for ICAM1 (PDB: 1MQ8); (size\_x = 21.936 Å, size\_y = 24.091 Å, and size\_z = 24.834 Å) for GAPDH (PDB: 1U8F); (size\_x = 23.317 Å, size\_y = 22.669 Å, and size\_z = 33.008 Å) for EGF (PDB: 1NQL); and (size\_x = 18.110 Å, size\_y = 25.507 Å, and size\_z = 21.592 Å) for APOE (PDB: 1B68). For the purpose to achieve this, the Auto Dock tool (version 1.5.6) was utilized, with an exhaustiveness value of 8. Following the molecules selected, the "Toggle Selection Spheres" option in PyRx was implemented to define the active amino acid residues that would outline the cavity. Additionally, the identification of allosteric sites is applied by using PASSer and the grid box was positioned accurately to include all residues in the allosteric site<sup>24</sup>. Rather than orthosteric binding sites, allosteric sites were used for these targets to enhance selectivity and reduce off-target effects. Orthosteric sites are often highly conserved and may interfere with endogenous ligand binding, whereas allosteric pockets allow modulation of protein activity through conformational changes without competing with natural ligands. This strategy enables fine control over protein function and improved therapeutic specificity<sup>25</sup>. Following that, docking was used to find the binding affinity of the ligands on each target.

#### ADMET predictions

Subsequent to the molecular docking, the dexamethasone-derived molecule demonstrating the highest binding affinity for the target protein's allosteric site conducted *in silico* pharmacokinetic and toxicity assessment. ADMET (Absorption, Distribution, Metabolism, Excretion, and Toxicity) properties were estimated utilizing AI Drug servers (AI Drug Lab (smu.edu)<sup>26</sup> for evaluating central nervous system (CNS)-related pharmacokinetics. AI Drug server was selected because it integrates multiple deep learning and QSAR-based models trained on large, experimentally validated datasets, allowing simultaneous prediction of pharmacokinetics parameters within a single interface. Compared to traditional tools, AI Drug server provides higher prediction accuracy and rapid screening capability, which made it suitable for prioritizing drug-like dexamethasone derivatives in this study<sup>27</sup>. Priority was placed on assessing blood-brain barrier (BBB) permeability, a crucial determinant of therapy effectiveness for PD. Toxicity features including

hepatotoxicity, mutagenicity, and overall safety, were evaluated for comparing the AI generated molecule with dexamethasone.

#### Molecular dynamics (MD) simulation

The molecular dynamics (MD) simulation of two complexes, dexamethasone and an AI-derived compound found through molecular docking study with favorable pharmacokinetic for PD, was conducted using the GROMACS 2023 program<sup>28</sup>. The protein was parameterized with the CHARMM36 force field, whereas the ligands were parameterized with the CHARMM General Force Field (CGenFF)<sup>29,30</sup>. Subsequent to creating the topology file, all complexes and the unattached protein structures were positioned into a cubic simulation box, solubilized using the TIP3P water model, and neutralized with ions using a 0.15 M NaCl solution. The system was subsequently energy-minimized via the steepest descent approach to eliminate steric conflicts while maintaining a stable initial structure. The system was equilibrated at a temperature of 300 K and a pressure of 1 atm in NVT and NPT ensembles for 500 picoseconds (ps) each. A production MD simulation of 100 nanoseconds (ns) was conducted with a 2-femtosecond step, recording trajectories every 10 ps for analysis. The Parrinello-Rahman barostat and the V-rescale thermostat<sup>31,32</sup> were employed to sustain constant pressure and temperature. The radius of gyration (Rg), hydrogen bonds, solvent accessible surface area (SASA), root mean square deviation (RMSD), and root mean square fluctuation (RMSF) were determined from the generated trajectory utilizing the GROMACS 2023 software. The resultant data was presented with XMGrace (Version 5.1.25) to provide time-resolved graphs.

#### Free energy calculation using MM-PBSA

The Molecular Mechanics Poisson-Boltzmann Surface Area (MM/PBSA) method was employed to determine the binding free energies of complexes. A study has been conducted on the trajectory data from the last 100 frames of the 100 ns MD simulations. The gmx\_MMPBSA program was employed to calculate the components of binding free energy, which include van der Waals (VDWAALS), electrostatic (EEL), polar solvation (ENPOLAR), and non-polar solvation (EPB) factors<sup>33</sup>. The solvation energy (GSOLV) was calculated by integrating both polar and non-polar solvation contributions, while the gas-phase interaction energy (GGAS) was determined by summing VDWAALS and EEL. The solvation energy (GSOLV) was calculated by integrating both polar and non-polar

solvation contributions, while the gas-phase interaction energy (GGAS) was determined by summing VDWALS and EEL. The GGAS and GSOLV components have been aggregated to determine cumulative binding free energy. In order to find critical amino acids that are involved in ligand binding, per-residue energy decomposition was employed. The Poisson–Boltzmann calculations were conducted using standard dielectric constants and solvent probe radii, and the AMBER force field parameters were aligned with the MD simulations.

## Results

### Intersection of parkinson's disease-associated genes and dexamethasone-responsive genes

The differential expression analysis of the GSE160299 dataset, which compared the plasma transcriptomes of PD patients and healthy controls, identified a total of 169 genes which reached the threshold of a fold change of at least 3 and an adjusted p-value of less than 0.05 (see Supplementary

Table S1). The volcano graph (see Supplementary Fig S1) indicates that these Differentially Expressed Genes (DEGs) comprised upregulated genes marked in red and downregulated genes marked in blue. The graph shows an individual pattern of gene expression changes, with various genes expressing significant upregulation or downregulation in PD patients comparing to healthy controls. CTD yielded 7728 dexamethasone-responsive genes. The Draw Venn Diagram tool had been used for conducting a Venn diagram analysis, which identified 92 overlapping genes that had similarities between the PD-associated DEGs and dexamethasone-responsive genes (Fig 1A). Enrichr's functional annotation platform demonstrated that the overlapping genes are primarily involved in molecular functions (Fig 1B) including cation binding, metal ion binding, retinoid binding, and monocarboxylic acid binding. This underscores the significance of metal ion homeostasis and ligand interactions in the potential mechanism of action of dexamethasone. Additionally, processes connected to

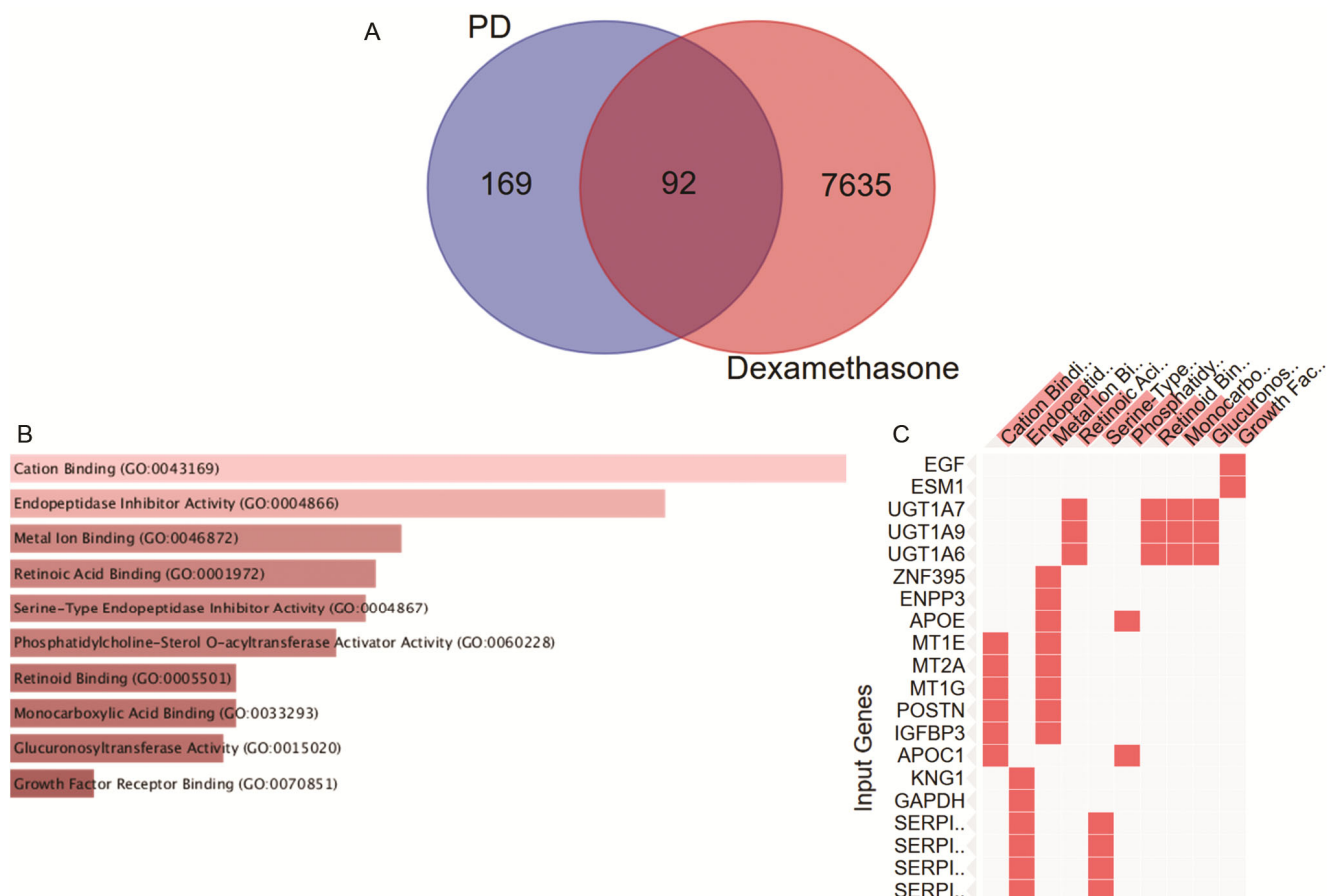


Fig. 1 — (A) Venn diagram is showing the overlap of dexamethasone-regulated genes in Parkinson's disease (PD) datasets; (B) Functional enrichment analysis highlighting key molecular functions, and (C) Clustergram identifying distinct gene clusters.

enzyme regulation, which include endopeptidase inhibitor action and serine-type endopeptidase inhibitor action, were also boosted, demonstrating an achievable role in regulating of protease function and processes of inflammation. Potential pathways through which dexamethasone could exert its beneficial effects in PD, including glucuronosyltransferase activity and growth factor receptor binding observed in this analysis. This implicates mechanisms such as retinoid signaling, enzyme regulation, and receptor-mediated pathways in its therapeutic action. The clustering of enriched molecular functions (Fig 1C) identified different categories of genes that may be associated with the effects of dexamethasone. Notably, the UGT family genes, which indicate a coordinated function in the metabolism of xenobiotics and glucuronidation. Furthermore, metallothioneins established a correlation associated with metal ion binding and detoxification processes. The intricate interplay of metabolic, inflammatory, and neuroprotective pathways modulated by dexamethasone in PD is corroborated by the involvement of additional critical genes, such as APOE, APOC1, IGFBP3, ESM1, EGF, and ZNF395.

#### Protein-Protein Interaction (PPI) Network Construction and Hub Gene Identification

An enrichment analysis was conducted using the intersecting genes in the Search Tool for the Retrieval of Interacting Genes (STRING) (Fig 2A). The average

number of neighbors in the STRING network was 10.6, with 91 nodes and 481 edges. The top 20 genes were selected by the CytoHubba plugin using the Maximum Neighborhood Component (MNC), Degree, Edge Percolated Component (EPC), Connection, and Radiality metrics. In (Fig 2B), the top 20 genes identified are LOX, EGF, ALB, CXCR4, APOE, CCND1, FLT1, GAPDH, SPP1, VCAM1, VWF, HMOX1, ICAM1, CD68, SCARB1, CD36, KDR, SPARC, and SERPINE1. We identified the CytoHubba genes as hub genes for additional bioinformatics analysis.

#### Gene ontology (GO) and functional enrichment analysis of hub genes

For the purpose of obtaining the biological process (BP), cellular compartment (CC), and molecular function (MF) (see SupplementaryTable S2), the official hub gene symbols were inputs into the Database for Annotation, Visualization, and Integrated Discovery (DAVID). For each category, only statistically significant terms ( $P < 0.05$ ) were included: 37 biological processes (BPs), 43 cellular components (CCs), and 9 molecular functions (MFs) (see Supplementary Table S3). The 9 most enriched terms in each category are displayed in the enrichment bubble plot (Fig 3A). This enrichment analysis reveals the significant connection of the dataset with extracellular and secretory processes, clearly identifying APOE as a crucial

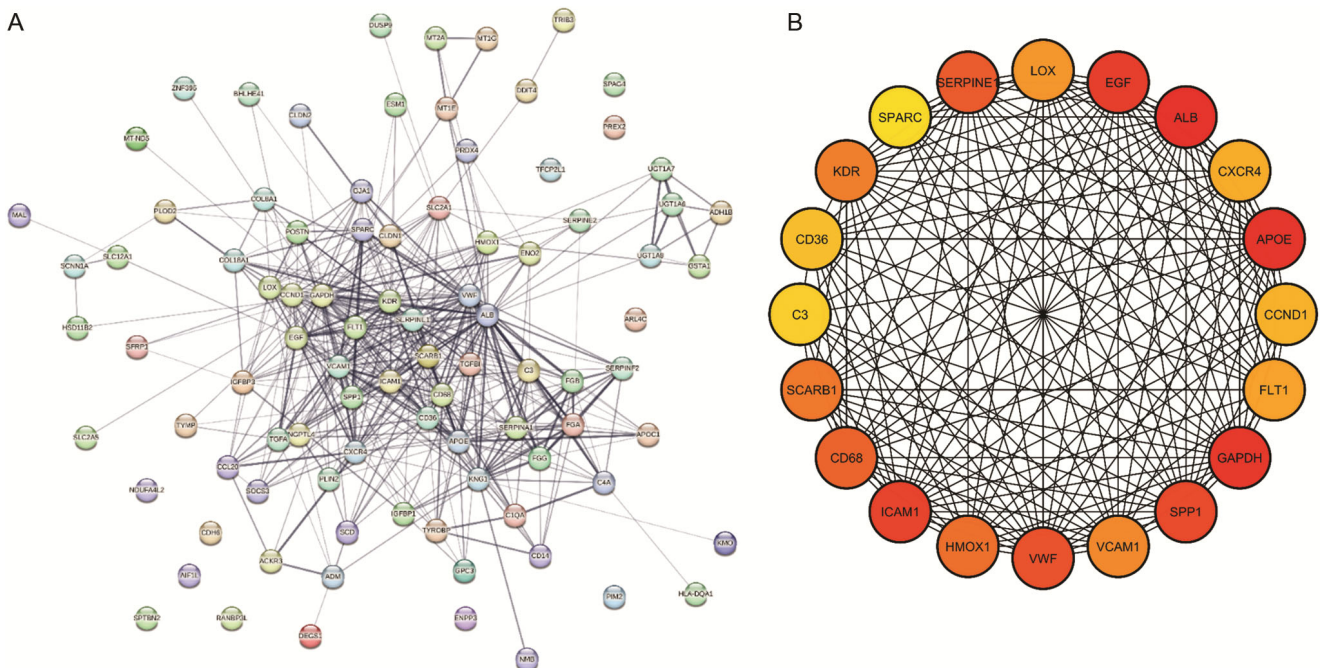


Fig. 2 — (A) STRING PPI network of PD and Dexamethasone intersection targets; (B) Top 20 hub genes identified by Cyto Hubba.

contributor. The most significant terms, extra-cellular space, secreted, glycoprotein, and extracellular exosome underscore APOE's function as a glycosylated, secreted protein implicated in lipid transport and cellular signaling<sup>34</sup>. In addition, the physiological significance of APOE in remodeling of vessels and cellular adhesion is underscored by terminology that includes positive modulation of angiogenesis and integrin binding<sup>35</sup>. The enrichment bubble diagram (Fig 3B) shows the ten most enriched Reactome pathways. The most significant aspect regarding this enrichment result is how it changed the architecture of the extracellular matrix (ECM), which can make  $\alpha$ -synuclein accumulate and enhance the neuron sensitivity<sup>36</sup>. APOE's role in eliminating

$\alpha$ -synuclein can have a significant impact on these processes<sup>37</sup>. ICAM1, which is linked to the integrin signaling and scavenger receptor pathway, can also disrupt the BBB and cause neuroinflammation<sup>38</sup>. GAPDH is linked to post-translational phosphorylation and platelet degranulation, which shows that it is involved in  $\alpha$ -synuclein pathology and oxidative stress<sup>39</sup>. EGF, on the other hand, is linked to receptor tyrosine kinase signaling and can affect the survival of neurons<sup>40</sup>.

#### AI dexamethasone modeling

WDDAICA platform was used to generate 10 dexamethasone derivatives, which are referred to as molecules A-J (Fig 4). Dexamethasone sites of the

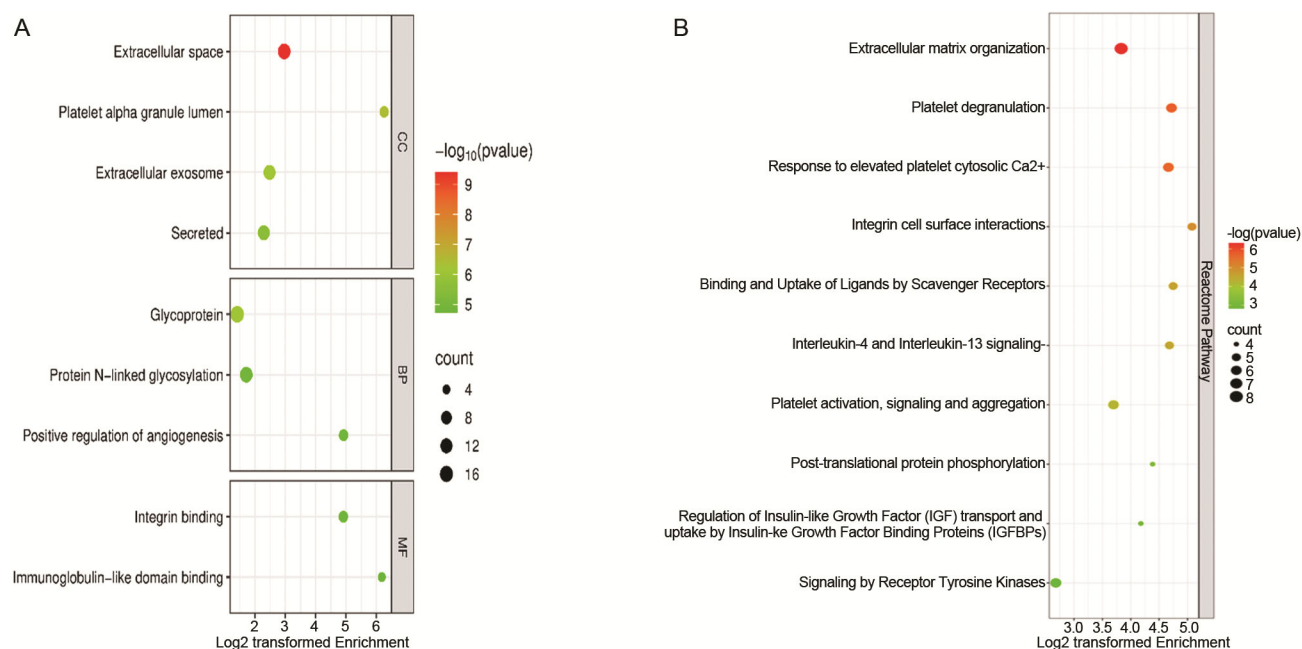


Fig. 3 — (A) Enrichment bubble plot of top 9 enriched BPs, CCs, and MFs; (B) Top 10 reactome pathways plotted in enrichment bubble.

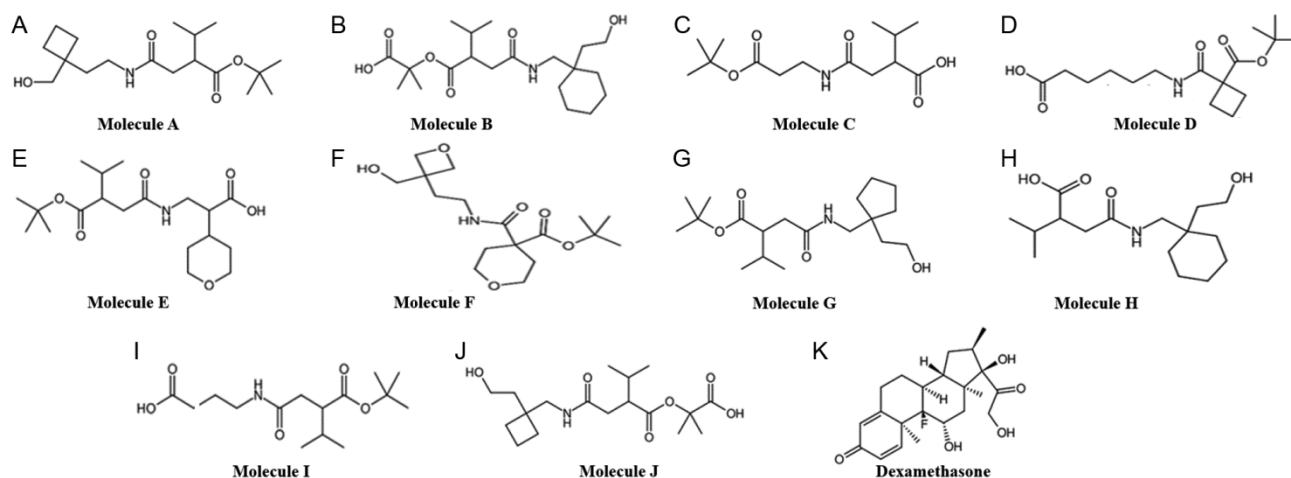


Fig. 4 — Novel dexamethasone analogues generated by AI for targeting PD pathogenesis.

core scaffold, the derivative structures exhibit distinct alterations at the C6 (Molecule A – C), C9 (Molecules D – F), and C21 (Molecule G – I) positions. Furthermore, molecule J exhibits a hybrid change at the C6, C9, and C16 positions. With the aim to minimize substantial glucocorticoid side effects while maintaining anti-inflammatory efficiency, as shown in molecules B and E, as well as the unique carbamate links in molecules G and H.

#### Molecular docking

The virtual screening analysis of the ten dexamethasone derivatives (Molecules A-J) showed that the investigated compounds had different binding affinities for four target proteins: ICAM1, GAPDH, EGF, and APOE. The values ranged from -7.6 kcal/mol to -4.6 kcal/mol (Table 1). Molecule C showed the highest binding affinity for APOE (-7.6 kcal/mol), which is close to the dexamethasone (-7.2 kcal/mol). The binding affinity of molecule I for ICAM1 was the lowest at -4.6 kcal/mol. Also, Molecule B and E both demonstrated favorable interactions with GAPDH (-6.5 kcal/mol). Based on the binding affinity results dexamethasone and molecule C on APOE were selected for further investigation. The 3D binding configuration shows that both dexamethasone and molecule C occupied similar spots of APOE (Fig 5A). Furthermore, the 2D interaction analysis of dexamethasone and molecule C with APOE (Fig 5A and B) reveals distinct binding profiles that may influence APOE's pathological role in PD. Dexamethasone engages in multiple interactions, including conventional hydrogen bonds with ASP153 and carbon hydrogen bonds with GLY31, extensive van der Waals contacts with residues such as LEU149, GLY31, and TRP34, and even an unfavorable acceptor interaction with GLN156. Molecule C, on the other hand, forms

hydrogen bonds with ASP153 and GLN156 and van der Waals bonds with ALA152, GLY31, and LEU28. Furthermore, both Ligands shows hydrophobic alkyl and pi-Alkyl interactions that further stabilize the binding through non-polar complementarity<sup>41</sup>.

#### ADMET predictions

ADMET profiling plays a crucial role in the drug discovery<sup>42</sup>. Comprehensive evaluation of pharmacokinetic and toxicity parameters makes it possible to rank drugs with good profiles, which helps avoid failures later in development stages. The current study shows that both dexamethasone and molecule C have acceptable molecular weights (MW) which are important for better oral bioavailability and cellular permeability. Molecule C (287.17 g/mol) has lower MW than dexamethasone (392.2 g/mol) (Table 2), which is an indicator for better absorption kinetics and membrane permeability<sup>43</sup>. Absorption, dexamethasone has a moderate human intestinal absorption (HIA) rate of 71.12%. Molecule C has a slightly lower rate of 60.68%, but it is still within an acceptable range for oral administration. Importantly, Molecule C has a greater estimated oral bioavailability (52.14%) compared to 36.5% for dexamethasone, which is a significant benefit because it indicates lower doses will have more predictable systemic exposure<sup>44</sup>. Regarding the solubility and permeability evaluations both drugs have moderate projected Caco-2 cell permeability, suggesting they could potentially cross the gut epithelium<sup>45</sup>.

Distribution indicates that both compounds are in the acceptable range for BBB permeability ( $\leq 30\%$ ), however molecule C (27.03%) is expected to penetrate marginally better than dexamethasone (18.52%). This property is very helpful since CNS-active drugs need to reach therapeutically relevant levels in the brain. Additionally, both

Table 1 — Binding affinity (kcal/mol) of dexamethasone and its novel AI analogues.

Ligand	Target	Binding Energy	Target	Binding Energy	Target	Binding Energy	Target	Binding Energy
AI Molecule A	APOE	-5.6	EGFR	-5.4	GAPDH	-5.8	ICAM1	-5.4
AI Molecule B	APOE	-6	EGFR	-6.4	GAPDH	-6.5	ICAM1	-5.1
AI Molecule C	APOE	-7.6	EGFR	-4.8	GAPDH	-5.7	ICAM1	-5.4
AI Molecule D	APOE	-6.7	EGFR	-5.4	GAPDH	-6.1	ICAM1	-5.2
AI Molecule E	APOE	-6.3	EGFR	-5.6	GAPDH	-6.5	ICAM1	-5.3
AI Molecule F	APOE	-6	EGFR	-5.3	GAPDH	-6	ICAM1	-5.6
AI Molecule G	APOE	-6.2	EGFR	-5.4	GAPDH	-6.4	ICAM1	-5
AI Molecule H	APOE	-6.5	EGFR	-5.4	GAPDH	-6	ICAM1	-5.5
AI Molecule I	APOE	-5.9	EGFR	-5.2	GAPDH	-5.9	ICAM1	-4.6
AI Molecule J	APOE	-6.2	EGFR	-5.4	GAPDH	-6.1	ICAM1	-5.1
Dexamethasone	APOE	-7.2	EGFR	-7.1	GAPDH	-7.1	ICAM1	-6.2

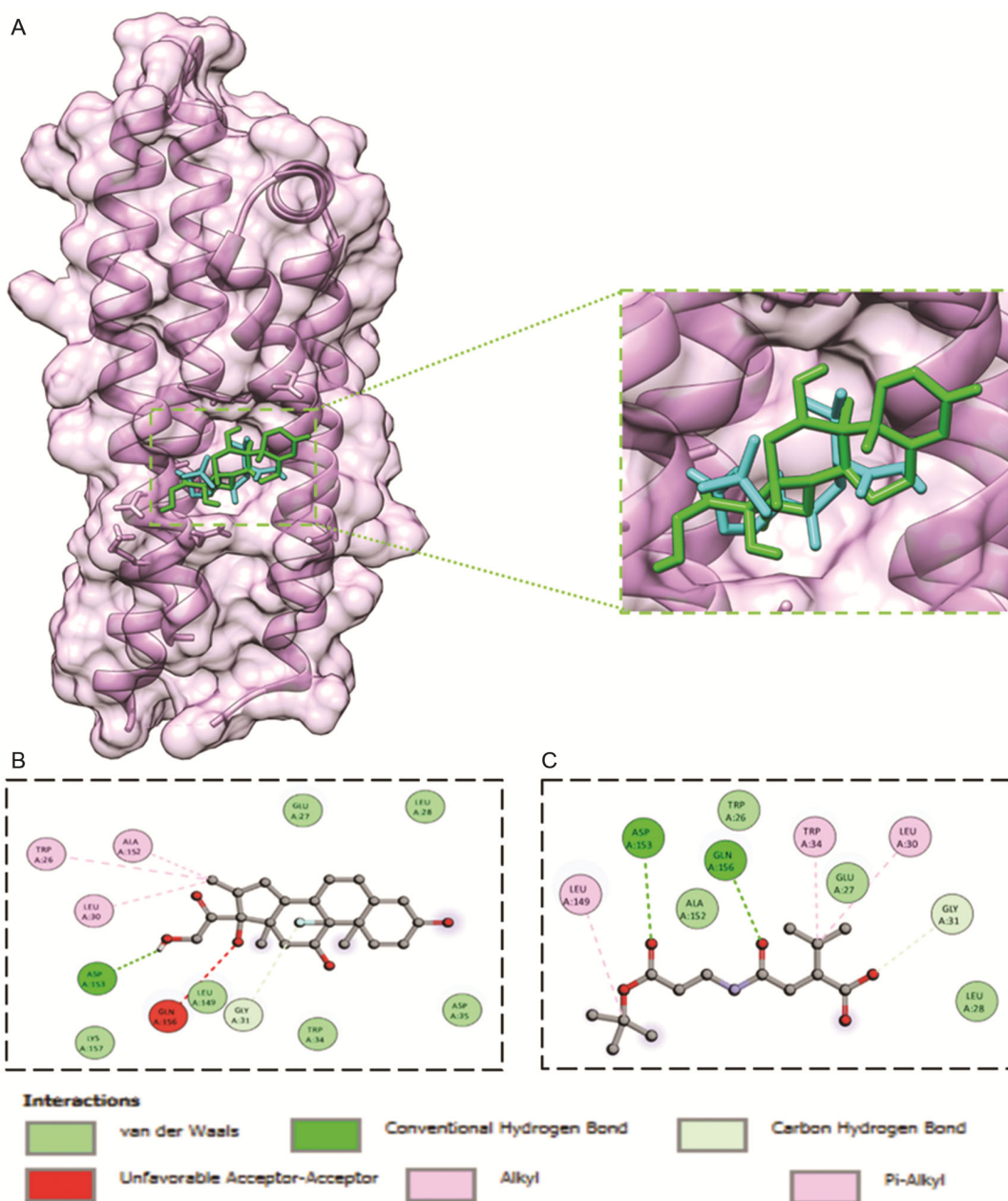


Fig. 5 — Molecular docking of compounds against APOE. (A) The 3D binding configuration of Dexamethasone (Green); Molecule C (Cyan). Both ligands occupied similar spots of our protein target. The molecular interaction fingerprints in 2D showed that atoms of Dexamethasone (B) and Molecule C (C) interacted with amino acid residues important for binding with APOE.

compounds have almost the same amount of plasma protein binding (PPBR), which means that there is a balanced amount of unbound, pharmacologically active drug in the blood<sup>46</sup>.

Metabolic profile shows concerns, especially when it involves blocking the cytochrome P450 enzyme. Both compounds are expected to moderately inhibit CYP2D6, but molecule C is expected to inhibit CYP2D6 considerably greater (93.41%). Toxicity estimations demonstrate that the overall safety profile

is comparable, however there are minor differences. Both compounds have similar general toxicity projections, but molecule C has a higher estimated risk of drug-induced liver injury (DILI) with 58.29% compared to the dexamethasone (34.64%). DILI is one of the primary reasons why the novel compounds fail in the clinical trials<sup>47</sup>, thus this result shows the significance of doing further research regarding the possibility of changing the structure to lower the risk of liver damage. In brief, molecule C appears to be an

Table 2 — ADMET profile of dexamethasone and molecule C using AI-drug lab.

Molecular Property	Optimal Range	Dexamethasone	Molecule C
Molecular Weight (kg/mol)	100~600	392.2	287.17
Number of Heteroatoms	1~15	6	6
Number of Rotatable Bonds	<=11	2	7
Number of Rings	<=6	4	0
Number of HA	<=12	5	4
Number of HD	<=7	3	2
<b>Absorption</b>			
Caco-2 Permeability (log(cm/s))	>-5.15	-5.07	-5.15
HIA (%)	Poor: <=30, Medium: 30~80, Optimal: >=80	71.12	60.68
Pgp Inhibition (%)	Optimal: <=30, Medium: 30~70, Poor: >=70	30.73	29.11
Oral Bioavailability (%)		36.5	52.14
<b>Distribution</b>			
BBB (%)	Optimal: <=30, Medium: 30~70, Poor: >=70	18.52	27.03
PPBR (%)	Optimal: <=90, Poor: >90	52.27	51.37
<b>Metabolism</b>			
CYP2C9 Inhibition (%)		43.89	38.64
CYP2D6 Inhibition (%)		84.39	93.41
CYP3A4 Inhibition (%)		30.29	33.9
CYP2C9 Substrate (%)		28.49	37.68
CYP2D6 Substrate (%)		48.58	57.19
CYP3A4 Substrate (%)		36.53	39.38
<b>Excretion</b>			
Half-Life (hr.)		53.48	55.75
<b>Toxicity</b>			
DILI (%)	Optimal: <=30, Medium: 30~70, Poor: >=70	34.64	58.29

appropriate candidate for further investigation since it has better oral bioavailability and BBB penetration than Dexamethasone. However, there are significant difficulties ahead, such as its high risk of DILI.

#### Molecular Dynamics (MD) simulation of APOE-compound complexes

Following performing molecular docking studies and ADMET profiling, we utilized GROMACS 2023 to perform a 100 ns molecular dynamics simulation to gain insight into the stability and dynamic behavior of APOE-compound complexes. The comparative MD simulation study provides us with an extensive amount of beneficial knowledge about how dexamethasone and Molecule C affect the structural dynamics of APOE in different ways. The root mean square deviation (RMSD) (Fig 6A) shows that molecule C has a considerably more stable structure than dexamethasone. In the beginning, dexamethasone maintains the structure stable, but after around 65 ns, it begins to change significantly, reaching a peak over 1.5 nm at around 75 ns, which shows that the binding stability is disrupted. The RMSD of molecule C remains about 0.5 nm during the simulation, which shows that the binding conformation in the APOE binding cavity is

stable and maintained effectively. (Fig 6B) which shows the root mean square fluctuation (RMSF), supports the idea that both dexamethasone and molecule C have similar profiles of flexibility at the residue level. However, around atom 1000, there is a clear difference: the dexamethasone complex has much higher RMSF values than molecule C, which reflects that this location is more flexible. The radius of gyration (Rg) (Fig 6C) shows that molecule C has a consistently lower Rg than dexamethasone, which suggests that molecule C makes APOE more compact overall. Furthermore, solvent accessible surface area (SASA) data (Fig 6D) shows that dexamethasone keeps a structure that is more exposed to solvents, whereas Molecule C lets the surface less exposed, which stands with its role in encouraging a more folded and hydrophobically protected shape. The hydrogen bond analysis (Fig 6E) shows that both dexamethasone and molecule C form about the same number of hydrogen bonds with APOE over the 100 ns simulation. The number of hydrogen bonds at all times ranged from 0 to 4. However, in the first 10 ns, dexamethasone has a few more hydrogen bonds than molecule C. This implies that there is an advantage in the total number of hydrogen

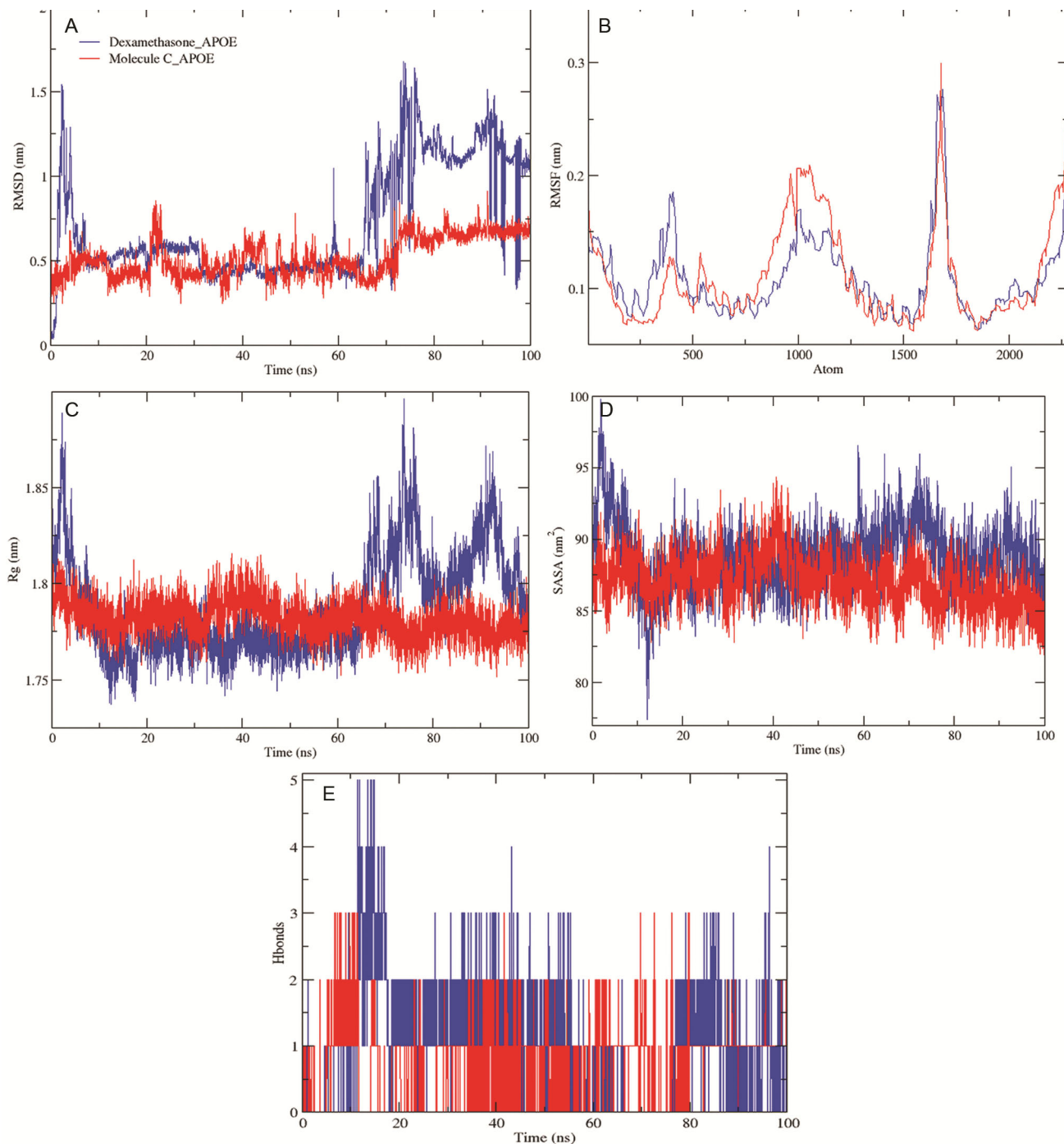


Fig. 6 — Molecular dynamics (MD) simulation of APOE, dexamethasone (blue), and molecule C (red) over a simulation run of 100 ns. (A) RMSD; (B) RMSF; (C) Rg; (D) SASA and (E) Number of Hydrogen bonds.

bonds. These results show that molecule C not only binds to APOE more stably, but it also makes the structure more compact.

#### Analysis of free energy calculation by MM-PBSA

Free energy calculation provides necessary information about how dexamethasone and molecule C

bind and interact with APOE. Molecule C has a total binding free energy of  $-13.8$  kcal/mol, which is better than dexamethasone ( $-1.8$  kcal/mol) (Table 3). The variance is primarily due to stronger VDWAALS  $-22.49$  kcal/mol for molecule C and  $-10.49$  kcal/mol for dexamethasone. This suggests that the APOE

Table 3 — Binding free energy (kcal/mol) calculations using MM/PBSA.

Compounds	VDWAALS	EEL	EGB	ENPOLAR	GGAS	GSOLV	TOTAL
Dexamethasone	-10.49 ± 1.96	-65.45 ± 30.1	75.7 ± 32.09	-1.57 ± 0.2	-75.94 ± 31.02	74.13 ± 31.98	-1.8 ± 3.26
Molecule C	-22.49 ± 2.59	-7.12 ± 7.75	18.44 ± 6.09	-2.63 ± 0.2	-29.61 ± 8.34	15.81 ± 6.05	-13.8 ± 3.51

Mean ± standard deviation (SD)

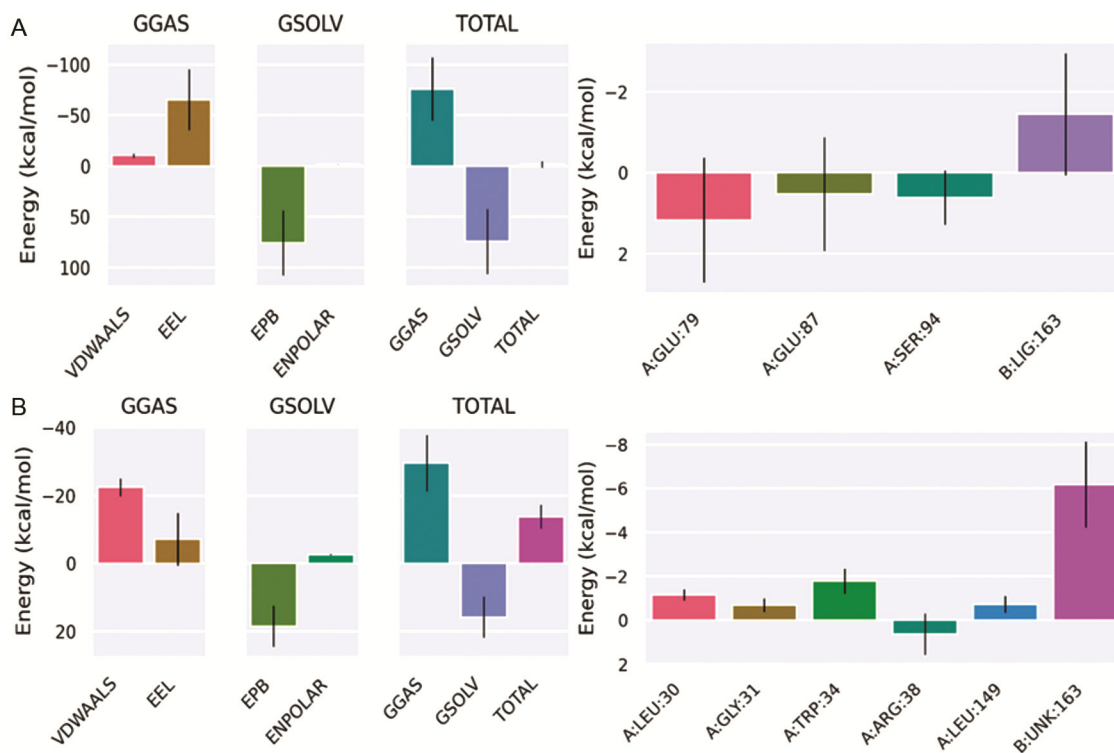


Fig. 7 — MM/PBSA analysis (left) binding free energy contribution by various interactions, (right) binding free energy contribution by active residues and ligand. (A) Dexamethasone and (B) Molecule C.

binding pocket has better hydrophobic packing and shape complementarity. Both compounds have EEL and ENPOLAR. However, Molecule C has a better overall GGAS (-29.61 kcal/mol) than dexamethasone (-75.94 kcal/mol), which implies the binding site has more balanced non-bonded interactions. The GSOLV for molecule C is significantly lower (15.81 kcal/mol) than for dexamethasone (74.13 kcal/mol). The per-residue energy decomposition data reveal even more differences in how the binding sites interact. The strongest stabilizing contributions to dexamethasone (Fig 7A) come from residues such as GLU79 and GLU87, which have fewer relevant interactions overall. In contrast, molecule C (Fig 7B) interacts with a broader range of residues throughout the binding surface, including LEU30, GLY31, TRP34, ARG38, and LEU149, all of which have strong stabilizing properties. This extensive and lasting association at the

residue level provides that molecule C binds to APOE more strongly and across an expanded region. The previously mentioned features may result in improved APOE stabilization, affecting its ability to bind to lipids and participate in neuroinflammation, both of which are hypothesized to have a role in the development of PD. Overall, these MM/PBSA results represent that molecule C is a more effective and selective APOE binder than dexamethasone.

## Discussion

This study shows that AI can contribute to discovering novel compounds for neurological disorders such as PD. Integrating transcriptome data with network pharmacology makes it achievable to find genes that are linked to both the pathology of PD and the therapeutic properties of dexamethasone. APOE, GAPDH, ICAM1, and EGF were identified as critical hub genes. Among them, APOE was identified

as the main target that was affected by dexamethasone and our AI-generated molecules, in addition to the role of APOE in  $\alpha$ -synuclein clearance, and neuroinflammation. Molecule C, an AI-analog of dexamethasone, has better affinity for APOE. Furthermore, MD simulations over 100 ns confirmed that the molecule C-APOE complex was more stable and compact than dexamethasone. Compared to dexamethasone, molecule C possessed a better ADMET profile, with higher BBB permeability and oral bioavailability, which are both important for drugs aimed to target the CNS. However, elevated the risk of hepatic damage necessitates modulation in molecule C structure. Substituting the carboxylic acid group with safer bioisosteres such as tetrazole or oxadiazolone may prevent reactive acyl-glucuronide formation, while replacing bulky tert-butyl groups with smaller alkyl or cycloalkyl moieties can improve metabolic stability. These changes can lower the risk of DILI associated with molecule C. The free energy analysis via MM-PBSA confirmed the better binding energy of molecule C, characterized by higher levels of van der Waals and electrostatic contributions. Per-residue decomposition indicated a more extensive and profound interaction with APOE than with dexamethasone, implying the possibility of greater control of APOE's neuroprotective pathways. The current study provides an encouraging strategy that observed a novel AI-derived compound which performs better than dexamethasone for targeting critical gene in PD. Although the *in silico* results appear promising, it remains essential to demonstrate efficacy by *in vitro* experiments. This strategy can be used for various neurological disorders, which could result in more effective therapies.

### Conclusion

This study effectively demonstrates the application of AI in the design of novel dexamethasone derivatives for possible therapeutic applications in PD. The integration of AI within WADDAICA markedly accelerates the drug design process and enhances candidate selection compared with conventional *in silico* approaches. This allows efficient identification of high-affinity molecules while reducing redundant docking iterations and computational cost, ultimately improving hit-to-lead success and design throughput. Through the integration of transcriptomic data, network pharmacology, molecular docking, ADMET profiling, MD simulation, and MM-PBSA free energy

calculations, we identified molecule C as a promising candidate exhibiting superior pharmacokinetic properties, enhanced binding affinity, and increased structural stability in its interaction with the APOE protein. Molecule C demonstrated superior oral bioavailability and BBB permeability in comparison to dexamethasone, which is essential for the development of drugs that targeting brain. The MM-PBSA results further validated its superior and more stable affinity for APOE. However, the necessity of structural modification of molecule C is underscored by the potential risk of hepatic injury. The utilization of AI in our *in silico* study offers an important platform for improving the development of next-generation neuroprotective drugs targeting complex disorders include PD. However, *in vitro* and *in vivo* investigations are needed to confirm that molecule C is a safe and effective compound.

### Acknowledgment

The authors express their profound appreciation to His Excellency Dr. Tariq bin Abdullah Al-Sheddi for his outstanding leadership and significant contributions to computing, artificial intelligence, and bioinformatics. As an early pioneer in these fields in the Kingdom of Saudi Arabia, his commitment and assistance have motivated and enabled researchers across the nation.

### Author Contributions

All authors contributed to the study conception and design. Material preparation, data collection, and analysis were performed by M.M.A., N.A., A.S.A. and A.A.A. (molecular docking, molecular dynamics simulation, and free energy calculation), A.F.A. and A.M.A. (ADMET prediction), N.G.A., F.A.A. and F.M.A. (AI-derived analogs generation), M.S.K. and F.A.A. (network pharmacology analysis). The first draft of the manuscript was written by Mohammed M. Alshehri, and all authors commented on previous versions of the manuscript. All authors read and approved the final manuscript.

### Declarations

Not to declare

### Funding

No funding was received for this research.

### Competing interest

The authors declare no conflict of interest.

**Ethics approval and Consent to participate**

Not applicable

**Consent for publication**

Not applicable

**Availability of data and material**

All data and materials will be made available upon reasonable request.

**References**

- Raza C, Anjum R & Shakeel NUA. Parkinson's disease: Mechanisms, translational models and management strategies. *Life Sci*, 226 (2019) 77.
- World Health Organization. Parkinson disease. (2023).
- Hirsch EC & Hunot S. Neuroinflammation in Parkinson's disease: a target for neuroprotection? *Lancet Neurol*, 8 (2009) 382.
- Block M, Zecca L & Hong JS. Microglia-mediated neurotoxicity: uncovering the molecular mechanisms. *Nat Rev Neurosci*, 8 (2007) 57.
- Billingsley KJ, Bandres-Ciga S, Saez-Atienzar S & Singleton AB. Genetic risk factors in Parkinson's disease. *Cell Tissue Res*, 373 (2018) 9.
- Khanna A, Adams J, Antoniadis C, Bloem BR, Carroll C & Cedarbaum J. Accelerating Parkinson's Disease drug development with federated learning approaches. *NPJ Parkinsons Dis*. 10 (2024) 225.
- Kurkowska-Jastrzebska I, Litwin T, Joniec I, Ciesielska A, Przybylkowski A, Członkowski A & Członkowska A. Dexamethasone protects against dopaminergic neurons damage in a mouse model of Parkinson's disease. *Int Immunopharmacol*. 10 (2004) 1307.
- Coutinho AE & Chapman KE. The anti-inflammatory and immunosuppressive effects of glucocorticoids, recent developments and mechanistic insights. *Mol Cell Endocrinol*. 335 (2011) 2.
- Beric A, Cisterna-García A, Martin C, Kumar R, Alfradique-Dunham I & Boyer K. Plasma acellular transcriptome contains Parkinson's disease signatures that can inform clinical diagnosis. *medRxiv*, 2024 (2024) 24315717.
- The Comparative Toxicogenomics Database (CTD).
- Oliveros JC, (2007–2015) Venny: an interactive tool for comparing lists with Venn's diagrams.
- Chen EY, Tan CM, Kou Y, Duan Q, Wan Z & Ma'ayan A. Enrichr: interactive and collaborative HTML5 gene list enrichment analysis tool. *BMC Bioinformatics*, 14 (2013) 128.
- Szklarczyk D, Kirsch R, Koutrouli M, Nastou K, Mehryary F, Hachilif R, Gable AL & Fang T. The STRING database in 2023: protein–protein association networks and functional enrichment analyses for any sequenced genome of interest. *Nucleic Acids Res*, 51 (2023) D638.
- Shannon P, Markiel A, Ozier O, Baliga NS, Wang JT, Ramage D, Amin N, Schwikowski B & Ideker T. Cytoscape: a software environment for integrated models of biomolecular interaction networks. *Genome Res*, 13 (2003) 2498.
- Sherman BT, Hao M, Qiu J, Jiao X, Baseler MW, Lane HC, Imamichi T & Chang W. DAVID: a web server for functional enrichment analysis and functional annotation of gene lists (2021 update). *Nucleic Acids Res*, 50 (2022) W216.
- Huang DW, Sherman BT & Lempicki RA. Systematic and integrative analysis of large gene lists using DAVID bioinformatics resources. *Nat Protoc*. 4 (2008) 44.
- Tang D, Chen M, Huang X, Zhang G, Zeng L, Zhang G, Wu S & Wang Y. SRplot: A free online platform for data visualization and graphing. *PLoS ONE*. 18 (2023)e0294236.
- Bai Q, Ma J, Liu S, Xu T, Banegas-Luna AJ, Pérez-Sánchez H, Tian Y, Huang J, Liu H & Yao X. WADDAICA: A webserver for aiding protein drug design by artificial intelligence and classical algorithm. *Comput Struct Biotechnol J*, 19 (2021) 3573.
- Bai Q. Research and development of MolAICal for drug design via deep learning and classical programming. *arXiv*. (2020)
- Rappe AK, Casewit CJ, Colwell KS, Goddard WA & Skiff WM. UFF, a full periodic table force field for molecular mechanics and molecular dynamics simulations. *J Am Chem Soc*, 114 (1992) 10024.
- Fasman GD. Prediction of protein structure and the principles of protein conformation. *Springer eBooks*, (1989) 1.
- Dallakyan S & Olson AJ. Small-Molecule Library Screening by Docking with PyRx. *Methods Mol Biol*, 1263 (2015) 243.
- Trott O & Olson AJ. AutoDock Vina: improving the speed and accuracy of docking with a new scoring function, efficient optimization, and multithreading. *J Comput Chem*, 31 (2010) 455.
- Tian H, Xiao S, Jiang X & Tao P. PASSer: fast and accurate prediction of protein allosteric sites. *Nucleic Acids Res*, 51 (2023) W427.
- Nussinov R & Tsai C. Allostery in disease and in drug discovery. *Cell*, 153 (2013) 293.
- AI Drug Lab. Southern Methodist University, Tao Research Group.
- Paul D, Sanap G, Shenoy S, Kalyane D & Tekade RK. Artificial intelligence in drug discovery and development. *Drug disco today*, 26 (2020) 80.
- Abraham MJ, Murtola T, Schulz R, Pál S, Smith JC, Hess B & Lindahl E. GROMACS: High performance molecular simulations through multi-level parallelism from laptops to supercomputers. *SoftwareX*, 1 (2015)1.
- Best RB, Zhu X, Shim J, Lopes PE, Mittal J, Feig M & Mackerell AD Jr. Optimization of the additive CHARMM all-atom protein force field targeting improved sampling of the backbone  $\phi$ ,  $\psi$  and side chain  $\chi_1$  and  $\chi_2$  dihedral angles. *J Chem Theory Comput*, 8 (2012) 3257.
- Vanommeslaeghe K, Hatcher E, Acharya C, et al. CHARMM General Force Field: A force field for drug-like molecules compatible with the CHARMM all-atom additive biological force fields. *J Comput Chem*. 31 (2010) 671.
- Parrinello M & Rahman A. Polymorphic transitions in single crystals: A new molecular dynamics method. *J Appl Phys*. 52 (1981) 7182.
- Bussi G, Donadio D & Parrinello M. Canonical sampling through velocity rescaling. *J Chem Phys*. 126 (2007) 014101.
- Darakjian B, Shuxing R & Thire T. gm\_x\_MMPBSA: a new tool to perform end-state free energy calculations in GROMACS. *J Chem Theory Comput*, 17 (2021) 6281.
- Mahley RW & Huang Y. Apolipoprotein E sets the stage: response to injury triggers neuropathology. *Neuron*, 76 (2012) 871.
- Laskowitz DT, Thekdi AD, Thekdi SD, Han SK, Myers JK, Pizzo SV & Bennett ER. Downregulation of microglial

- activation by apolipoprotein E and apoE-mimetic peptides. *Exp Neurol*, 167 (2001) 74.
- 36 Karpinar DP, Balija MBG & Kügler S. Pre-fibrillar  $\alpha$ -synuclein variants with impaired  $\beta$ -structure increase neurotoxicity in Parkinson's disease models. *EMBO J*, 28 (2009) 3256.
- 37 Zhao N, Attrebi ON, Ren Y, Qiao W, Sonustun B, Martens YA, Meneses AD, Li F, Shue F, Linares C, Chen Y, Delenclos, M, Liu C, Fryer JD & Bu G. APOE4 exacerbates  $\alpha$ -synuclein pathology and related toxicity independent of amyloid. *Science Translational Medicine*, 12 (2020) 529.
- 38 Yang C, Hawkins KE, Doré S & Candelario-Jalil E. Neuroinflammatory mechanisms of blood-brain barrier damage in ischemic stroke. *Am J Physiol Cell Physiol*, 316 (2019) C135.
- 39 Tristan C, Shahani N, Sedlak TW & Sawa A. The diverse functions of GAPDH: views from different subcellular compartments. *Cell Signal*, 23 (2011) 317.
- 40 Hefti F & Mash DC. Localization of nerve growth factor receptors in the normal human brain and in Alzheimer's disease. *Neurobiol Aging*, 10 (1989) 75.
- 41 Huey R, Morris GM, Olson AJ & Goodsell DS. A semiempirical free energy force field with charge-based desolvation. *J Comput Chem*, 28 (2007) 1145.
- 42 van de Waterbeemd H & Gifford E. ADMET in silico modelling: towards prediction paradise? *Nat Rev Drug Discov*, 2 (2003) 192.
- 43 Lipinski CA, Lombardo F, Dominy BW & Feeney PJ. Experimental and computational approaches to estimate solubility and permeability in drug discovery and development settings. *Adv Drug Deliv Rev*, 46 (2001) 3.
- 44 Fagerholm U, Hellberg S & Spjuth O. Advances in Predictions of Oral Bioavailability of Candidate Drugs in Man with New Machine Learning Methodology. *Molecules*, 26 (2021) 2572.
- 45 Artursson P & Karlsson J. Correlation between oral drug absorption in humans and apparent drug permeability coefficients in human intestinal epithelial (Caco-2) cells. *Biochem Biophys Res Commun*, 175 (1991) 880.
- 46 Pardridge WM. Drug transport across the blood-brain barrier. *J Cereb Blood Flow Metab*, 32 (2012) 1959.
- 47 Fu S, Wu D, Jiang W, Li J, Long J, Jia C & Zhou T. Molecular Biomarkers in Drug-Induced Liver Injury: Challenges and Future Perspectives. *Front Pharmacol*, 10 (2020) 1667.